

Sterically promoted zirconium–phosphorus π -bonding: structural investigations of $[\text{Cp}_2\text{Zr}(\text{Cl})\{\text{P}(\text{H})\text{Dmp}\}]$ and $[\text{Cp}_2\text{Zr}\{\text{P}(\text{H})\text{Dmp}\}_2]$ (Dmp = 2,6-Mes₂C₆H₃)

Eugenijus Urnėžius, Stephen J. Klippenstein, John D. Protasiewicz *

Department of Chemistry, Case Western Reserve University, Cleveland, OH 44106-7078, USA

Received 6 April 1999; accepted 14 June 1999

Abstract

The new terminal zirconocene–organophosphanido complexes $[\text{Cp}_2\text{Zr}(\text{Cl})\{\text{P}(\text{H})\text{Dmp}\}]$ (**1**) and $[\text{Cp}_2\text{Zr}\{\text{P}(\text{H})\text{Dmp}\}_2]$ (**2**) (Dmp = 2,6-Mes₂C₆H₃) bearing the sterically demanding ligand Dmp have been prepared and structurally characterized. A flattened pyramidal geometry for the phosphorus atom of **1** and a shortened Zr–P bond length of 2.638(1) Å provide evidence for moderate Zr–P π -bonding. Compound **2**, however, displays both pyramidal and planar phosphorus atoms. The corresponding Zr–P bond lengths of 2.726(2) and 2.519(2) Å, in conjunction with the phosphorus geometries, indicate that one phosphanido ligand is engaged in substantial π -bonding to the zirconium center while minimal, if any, of such interactions are present for the other phosphanido ligand. The solid state structures and ³¹P NMR spectra for **1** and **2** are very different than previously reported $[\text{Cp}_2\text{Zr}(\text{Cl})\{\text{P}(\text{H})\text{Mes}^*\}]$ and $[\text{Cp}_2\text{Zr}\{\text{P}(\text{H})\text{Mes}^*\}_2]$ (Mes* = 2,4,6-^tBu₃C₆H₂) which carry the related sterically demanding group Mes*. Comparisons to other structurally characterized zirconocene(IV) and hafnocene(IV) complexes having terminal phosphanido ligands suggest that upon increasing the steric congestion at the phosphorus atoms greater π interactions with the metal centers are afforded if such steric interactions do not prevent achieving proper alignment of the PR₂ group for optimal M–P π -bonding. © 2000 Elsevier Science S.A. All rights reserved.

Keywords: Crystal structures; Zirconium complexes; Metallocene complexes; Phosphanido ligand complexes

1. Introduction

Group IV metallocenes containing organophosphanido ligands (PR₂) have a rich and diversified chemistry [1]. Such materials have been investigated for applications in the synthesis of early–late heterobimetallic complexes [2]. In addition, these materials are active intermediates in catalytic PP-bond forming reactions [3,4]. More recently, attention has focused on the pursuit of related compounds having metal–phosphorus multiple bonds for utilization in phosphinidene transfer reactions [1,5–13]. In the present study we have prepared and structurally characterized two new

zirconocene–organophosphanido complexes, $[\text{Cp}_2\text{Zr}(\text{Cl})\{\text{P}(\text{H})\text{Dmp}\}]$ (**1**), and $[\text{Cp}_2\text{Zr}\{\text{P}(\text{H})\text{Dmp}\}_2]$ (**2**) (Dmp = 2,6-Mes₂C₆H₃). These materials were prepared during the course of our work to examine the chemistry of the zirconium phosphinidene complex $[\text{Cp}_2\text{Zr}=\text{PDmp}(\text{PMe}_3)]$ which also contains the sterically demanding Dmp group to render stability to Zr–P multiple bonds [14]. Recent structural work has unveiled novel molecular architectures for the alkali metal salts of DmpPH₂ [15,16]. Compounds **1** and **2** represent the first examples of structurally characterized transition metal complexes derived from this primary sterically encumbered phosphine. Analysis of structurally characterized Group IV metallocene complexes containing terminal phosphanido groups suggests that the geometry and π -bonding of terminal PR₂ groups may be largely dominated by steric factors.

* Corresponding author. Tel.: +1-216-368 5060; fax: +1-216-368 3006.

2. Experimental

All reactions were performed under a nitrogen atmosphere using Schlenk techniques, Vacuum Atmospheres' or Braun MB-150M dry boxes. DmpPH₂ was prepared as described previously [17]. Solvents were distilled from sodium/benzophenone solutions. ¹H NMR spectra were recorded on Varian Gemini 200 or 300 spectrophotometers and referenced to residual solvent ¹H signals. ³¹P NMR spectra were recorded on the Varian Gemini 300 instrument operating at 121.4 MHz and referenced to external 85% H₃PO₄. Elemental analyses were performed at Oneida Research Services, Whitesboro, NY.

2.1. Li[P(H)Dmp]·Et₂O

To a slurry of 1.56 g of DmpPH₂ (4.51 mmol) in 20 ml Et₂O were added 2.82 ml of 1.6 M ⁿBuLi (4.51 mmol) in hexanes. The resulting slurry was stirred for 30 min and the precipitate was filtered off and dried in vacuo for 1.5 h. The isolated pale-yellow Li[P(H)Dmp]·Et₂O (1.40 g, 74% yield) has one molecule of coordinated diethyl ether as ascertained by ¹H NMR spectroscopy. ¹H NMR (C₆D₆): δ 6.99 (t, J_{HH} = 7 Hz, 1H), 6.84 (d, J_{HH} = 7 Hz, 2H), 6.83 (s, 4H), 3.26 (q, J = 7 Hz, 4H), 2.21 (s, 6H), 2.12 (s, 12H), 1.06 (t, J = 7 Hz, 6H); P–H not observed. ³¹P NMR (C₆D₆): δ –145 (broad).

2.2. [Cp₂Zr(Cl){P(H)Dmp}] (1)

A solution of 0.401 g of Li[P(H)Dmp]·Et₂O (0.941 mmol) in 3 ml DME was added to a stirred solution of 0.380 g of [Cp₂ZrCl₂] (1.30 mmol) in 7 ml of DME. A deep-red color developed immediately. After stirring for 2 h the solution was filtered through a fritted glass filter and the solvent was removed under vacuum. Recrystallization at 0°C from hot toluene yielded 0.347 g of orange-red crystalline **1** (crude yield 61%, contaminated with trace amounts of **2** and [Cp₂ZrCl₂]). Further recrystallization does provide purer **1** but with appreciable losses in yield. ¹H NMR (C₆D₆): δ 7.06–7.00 (m, 3H), 6.95 (s, 4H), 5.58 (s, 5H), 5.57 (s, 5H), 4.60 (d, J_{HP} = 250 Hz, 1H), 2.30 (s, 12H), 2.22 (s, 6H). ³¹P NMR (C₆D₆): δ 25 (d, J_{HP} = 250 Hz). *Anal. Calc.* for C₃₄H₃₆ClPZr: C, 67.80; H, 6.02. Found: C, 67.27; H, 5.92%.

2.3. [Cp₂Zr{P(H)Dmp}₂] (2)

To a stirred solution of 0.355 g of Li[P(H)Dmp]·Et₂O (0.833 mmol) in 20 ml of toluene was slowly added a solution of 0.119 g of [Cp₂ZrCl₂] (0.411 mmol) in 20 ml toluene. The resulting deep-red solution was stirred for a further 45 min and then filtered through a fritted glass

filter. The volatiles were removed under vacuum to afford 0.439 g of deep-red impure **2**. ¹H NMR analysis (versus ferrocene) of this material revealed a maximal yield of 82% for **2**. Analytically pure samples were obtained by recrystallization from 6:1 hot hexanes–benzene solutions at –35°C. X-ray quality crystals were obtained by slow pentane diffusion into a saturated THF solution of [Cp₂Zr{P(H)Dmp}₂] at room temperature. ¹H NMR (C₆D₆): δ 7.02 (m, 2H), 6.94 (m, 4H), 6.88 (s, 8H), 5.28 (s, 10H), 3.70 (d, J_{HP} = 256 Hz, 2H), 2.26 (s, 12H), 2.17 (s, 24H). ³¹P{¹H} NMR (C₆D₆): δ 17.4 (br s). ³¹P NMR (C₆D₆): δ 17.4 (br d, J_{HP} = 256 Hz). *Anal. Calc.* for C₅₈H₆₂P₂Zr: C, 76.36; H, 6.85. Found: C, 76.16; H, 6.82%.

2.4. X-ray crystallography

Diffraction data were collected with a Siemens P4 instrument (Mo Kα radiation (λ = 0.71073 Å)). Crystals were mounted in the dry-box under nitrogen and sealed in 0.4 mm capillary tubes. Crystals were judged to be acceptable based on omega scans and rotation photography. A random search located reflections to generate the reduced primitive cell, and cell lengths were corroborated by axial photography. Additional reflections with 2θ values near 25° were appended to the reflection array and yielded the refined cell constants. Data were collected as presented in Table 1 and were corrected for absorption (empirical ψ scans). Examination on the diffractometer yielded monoclinic cells for both **1** and **2**.

Computations were performed using SHELXTL PLUS, Version 5 (Siemens Analytical) and data were refined against F² (wR₂ = Σ[w(F_o² – F_c²)²]/Σ[w(F_o²)²]^{1/2}). Systematic absences for **1** were consistent with the space group P2(1)/n. Systematic absences for **2** were consistent with the space group Cc. Refinement of the opposite enantiomorph of **2** resulted in higher R values (R₁ = 0.0471, wR₂ = 0.1061) and a higher absolute structure factor (0.37(6)). Most non-hydrogen atoms were located with direct methods, and the remaining non-hydrogen atoms were located in successive difference maps. All of the non-hydrogen atoms were refined anisotropically. For compound **1** all hydrogen atoms were located in successive difference maps and their positions refined. For compound **2** hydrogen atoms on the phosphorus atoms were located and positions refined, while remaining hydrogen atoms were generated at idealized positions.

2.5. Computation

Non-local density functional theory (DFT) was employed in the determination of the optimized structures and energies of [Cp₂Zr(H)PH₂] and [Cp₂Zr(Cl)PH₂]. These determinations employed the B3-LYP (Becke-3

Table 1
Crystal data and structure refinement for **1** and **2**

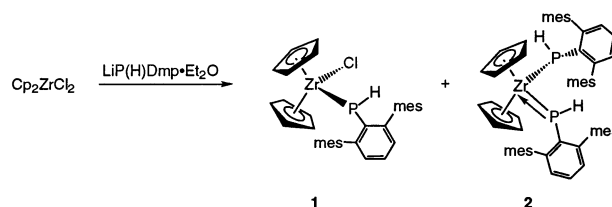
	1	2
Empirical formula	C ₃₄ H ₃₆ ClPZr	C ₅₈ H ₆₂ P ₂ Zr
Formula weight	602.27	912.24
Temperature (K)	293(2)	293(2)
Wavelength (Å)	0.71073	0.71073
Crystal system	monoclinic	monoclinic
Space group	<i>P</i> 2(1)/ <i>n</i>	<i>C</i> <i>c</i>
Unit cell dimensions		
<i>a</i> (Å)	10.3728(13)	19.742(3)
<i>b</i> (Å)	14.8103(14)	12.285(2)
<i>c</i> (Å)	19.5584(13)	22.598(3)
α (°)	90	90
β (°)	100.006(7)	115.114(9)
γ (°)	90	90
<i>V</i> (Å ³)	2958.9(5)	4962.4(16)
<i>Z</i>	4	4
<i>D</i> _{calc} (Mg m ⁻³)	1.352	1.221
Absorption coefficient (mm ⁻¹)	0.537	0.322
<i>F</i> (000)	1248	1920
Crystal size (mm)	0.36 × 0.36 × 0.16	0.36 × 0.30 × 0.12
Crystal color/shape	brown–orange/plate	red–brown/irregular
θ Range for data collection (°)	2.09–23.00	1.99–24.50
Limiting indices	–1 < <i>h</i> < 11, –1 < <i>k</i> < 16, –21 < <i>l</i> < 21	–1 < <i>h</i> < 22, –1 < <i>k</i> < 14, –26 < <i>l</i> < 24
Reflections collected	5356	4962
Independent reflections	4119 (<i>R</i> _{int} = 0.0308)	4494 (<i>R</i> _{int} = 0.0284)
Refinement method	full-matrix least-squares on <i>F</i> ²	full-matrix least-squares on <i>F</i> ²
Data/restraints/parameters	4119/0/443	4494/2/557
Goodness-of-fit on <i>F</i> ²	1.082	1.047
Final <i>R</i> indices [<i>I</i> > 2σ(<i>I</i>)]	<i>R</i> ₁ = 0.0401, <i>wR</i> ₂ = 0.0756	<i>R</i> ₁ = 0.0465, <i>wR</i> ₂ = 0.0921
<i>R</i> indices (all data)	<i>R</i> ₁ = 0.0743, <i>wR</i> ₂ = 0.0864	<i>R</i> ₁ = 0.0754, <i>wR</i> ₂ = 0.1045
Absolute structure parameter	na	0.01(5)
Extinction coefficient	0.0008(2)	0.00022(12)
Largest difference peak and hole (e Å ⁻³)	0.298 and –0.277	0.273 and –0.276

Lee–Yang–Parr) hybrid functional [18] and a 6-31G* basis set for the C and H atoms [19]. The LANL2DZ basis set, which includes the Hay and Wadt relativistic effective core potential, was employed for the Zr atoms [20]. GAUSSIAN94 quantum chemistry software was employed in these calculations [21].

3. Results and discussion

The addition of 1 equiv. of Li[P(H)Dmp]·Et₂O [17] to zirconocene dichloride in toluene rapidly leads to a deep blood-red solution containing a mixture of [Cp₂Zr(Cl){P(H)Dmp}] (**1**) and [Cp₂Zr{P(H)Dmp}₂] (**2**) (Scheme 1). The presence of both **1** and **2** was indicated by a pair of ³¹P NMR resonances at δ 23.1 ppm (d, *J*_{HP} = 250 Hz) and 18.0 ppm (d, *J*_{HP} = 257 Hz), respectively. ¹H NMR (C₆D₆) analysis of the material after removal of toluene under vacuum revealed an approximate equilibrium ratio of 1.0:1.6 for **1** to **2** (in addition to unreacted [Cp₂ZrCl₂]). The formation of **2** in preference to **1** was further exaggerated if [Cp₂ZrCl₂] was not fully dissolved prior to addition of Li[P(H)Dmp]·Et₂O.

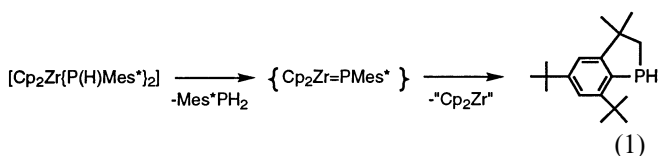
Likewise, addition of 0.5 equiv. of Li[P(H)Dmp]·Et₂O to [Cp₂ZrCl₂] results in a ratio of **1**:**2** of about 6.0:1.0. Compounds **1** and **2** are difficult to separate from [Cp₂ZrCl₂] and from one another by simple recrystallization when formed under these conditions. The propensity for the addition of two PR₂ groups to [Cp₂ZrCl₂] was somewhat diminished by performing the reaction in dimethoxyethane (DME). Addition of 1 equiv. of Li[P(H)Dmp]·Et₂O to [Cp₂ZrCl₂] in DME results in a ratio of 2.5:1.0 for **1**:**2**. Under the optimal conditions for formation of **1** (0.72 equiv. Li[P(H)Dmp]·Et₂O to [Cp₂ZrCl₂], DME), crude yields of 61% (contaminated by traces of **2** and [Cp₂ZrCl₂]) for **1** could be obtained. The reaction of **2** with



Scheme 1.

[Cp₂ZrCl₂] was explored as an alternative synthesis of **1**, but the resulting mixture still contained a distribution of species. Similar phosphanido redistributions and labile mixtures of mono- and bis-phosphanido zirconocenes have been observed for reactions of LiPPh₂ with [Cp₂ZrCl₂] [22].

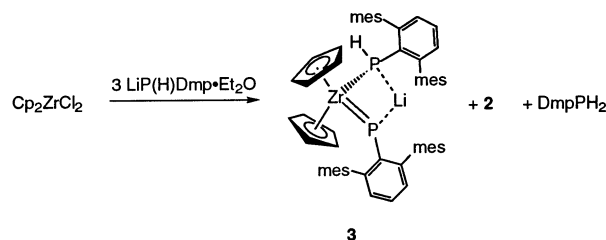
Isolation of the bis-phosphanido species **2** was optimized by increasing the amount of Li[P(H)Dmp]·Et₂O relative to [Cp₂ZrCl₂] to 2.1:1 and performing the reaction in toluene or benzene. Such reactions yielded **2** as the predominate species (ca. 82% yield by ¹H NMR). Invariably, traces of **1** and a third species (**3**) were also present and thus work-up required extensive recrystallization to purify **2** to a level sufficient for satisfactory elemental analysis. Once free of contaminants, compound **2** is extremely stable in solution in the absence of water and oxygen. In fact, solutions of pure **2** can be heated to 80°C (sealed NMR tube, C₆D₆) for hours with no signs of decomposition. This stability is in stark contrast to the related bis-phosphanido complex [Cp₂Zr{P(H)Mes*}₂], which could only be isolated as an impure material and in low yields owing to its tendency to undergo decomposition to Mes*PH₂ and the cyclometallation product derived from a zirconocene phosphinidene complex (eq. (1)) [23]. The postulated intermediate phosphinidene [Cp₂Zr=PMes*] has been trapped as the PMe₃ adduct [Cp₂Zr(=PMes*)(PMe₃)] [8,24–27]. The disparate stabilities of **2** and [Cp₂Zr{P(H)Mes*}₂] may be a result of the diverse nature of Zr–P bonding in the corresponding structures of these materials (see below), or an inability for **2** to attain conformations required for elimination of ArPH₂, or perhaps the presence of a more cyclometallation resistant ligand. Addition of PMe₃ to **2** in THF or toluene leads to slow formation of [Cp₂Zr(=PDmp)(PMe₃)] and DmpPH₂, albeit in low yields [28]¹.



Attempts to consume **1** completely by further increasing the ratio of Li[P(H)Dmp]·Et₂O to [Cp₂ZrCl₂] led to increasing amounts of **3** and DmpPH₂ that were also difficult to separate from **2** by recrystallization. Compound **3** displays ³¹P NMR signals at δ 496 (broad) and –103 ppm (dm, *J*_{HP} = 263 Hz)². The struc-

¹ Identified by NMR, preliminary X-ray structure analysis, and independent synthesis from [Cp₂Zr(Me)Cl] and LiP(H)Dmp.

² [Cp₂Zr=PDmp{DmpP(H)Li}] (**3**). ¹H NMR (C₆D₆): δ 7.11–7.00 (m, 3H), 6.93 (m, 1H), 6.89 (m, 4H), 6.82 (s, 2H), 6.77–6.74 (m, 4H), 5.49 (s, 10H), 2.40 (s, 6H), 2.27 (dm, *J*_{HP} = 261 Hz, 1H), 2.19 (m, 24H), 2.12 (s, 6H). ³¹P{¹H} NMR (toluene): δ 496 (br s), –103 (m). ³¹P NMR (toluene): δ 496 (br s), –103 (dm, *J*_{HP} = 263 Hz).



Scheme 2.

ture of **3** has tentatively been assigned as the anionic phosphinidene complex [Cp₂Zr=PDmp{LiP(H)Dmp}] (Scheme 2) based on comparisons to the ³¹P NMR of known anionic phosphinidene complexes ([Cp₂Zr=PMes*{K(H)(THF)₂}]₂ δ 565 ppm, and [Cp*₂Zr=PMes*{LiCl(DME)}] δ 537.6) and independent synthesis by reaction of **2** with 1 equiv. of ⁿBuLi. Unfortunately we have been unable, thus far, to isolate **3** as X-ray quality single crystals.

The structures of compounds **1** and **2** have been investigated by a pair of single-crystal X-ray diffraction experiments. For clarity of discussion, the results for **2** are presented first. Single crystals of **2** were grown by pentane diffusion into a saturated THF solution of **2**, and the results of the structural determination are presented in Fig. 1. The most significant and noteworthy features of **2** are the details regarding the Zr–P bonding. The Zr–P distances of 2.519(2) and 2.726(2) Å are very disparate (0.207 Å) and nearly span the whole range of known Zr–PR₂ bond lengths. The corresponding two phosphorus atoms display two very different geometries. The geometry at P1 is essentially planar as

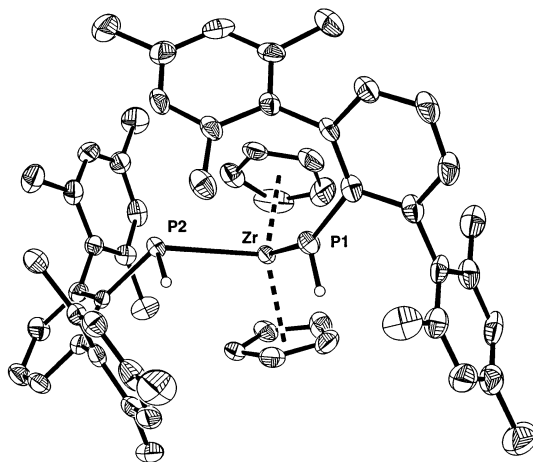
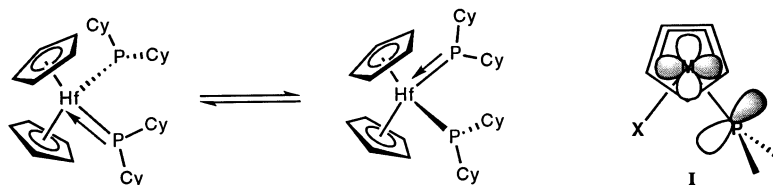


Fig. 1. Thermal ellipsoid plot for [Cp₂Zr{P(H)Dmp}₂] (**2**). Selected bond distances (Å) and angles (°): Zr–P1: 2.519(2), Zr–P2: 2.726(2), P1–H1: 1.17(8), P2–H2: 1.36(7), P1–Zr–P2: 91.30(7), Zr–P1–H1: 106(4), Zr–P1–C101: 142.8(3), C101–P1–H1: 109(4), Zr–P2–H2: 92(3), Zr–P2–C201: 121.4(2), C201–P2–H2: 88(3).



Scheme 3.

gauged by the sum of the bonds angles ($\Sigma_{\text{BA}}(\text{P1}) = 358(6)^\circ$), while the geometry at P2 is pyramidal ($\Sigma_{\text{BA}}(\text{P2}) = 301(4)^\circ$). These values are mirrored by Zr–P–C bond angles of $142.8(3)$ and $121.4(2)^\circ$, respectively. The interesting asymmetric environments exhibited by the two phosphanido ligands in **2** are reminiscent of the structure of $[\text{Cp}_2\text{Hf}(\text{PEt}_2)_2]$, the first example of a bis-phosphanido complex to exhibit this type of structural feature [29]. This particular structure contains both planar and pyramidal phosphorus atoms ($\Sigma_{\text{BA}}(\text{P1}) = 358.8(3)^\circ$) and ($\Sigma_{\text{BA}}(\text{P2}) = 311.9(3)^\circ$) and displays correspondingly short ($2.488(1)$ Å) and long ($2.682(1)$ Å) Hf–P bond lengths.

Adoption of a planar geometry for one of the phosphanido ligands in **2** or $[\text{Cp}_2\text{Hf}(\text{PEt}_2)_2]$ can be attributed to the desire for the complex to achieve an 18 valence electron count configuration. However, not all such Group IV metallocenes choose to adopt planar phosphanido groups to achieve an 18 valence electron count (as discussed below). A planar phosphanido group should also be aligned perpendicular to the plane of the three atoms in the wedge of the metallocene for optimal π -bonding to the a_1 π -accepting molecular orbital of the metallocene fragment (structure **I**, Scheme 3). The arrangement of the phosphanido unit in **2** is offset by 18° from this orientation for maximal π -bonding [30]. For some recent important discussions of ligand lone pair π -interactions with transition metal centers see Ref. [3].

The structure of compound **1** provides a comparison of the bonding of a single Dmp(H)P group to a zirconocene center. The details of the molecular environments for **1** are presented in Fig. 2. Again, the most interesting feature is the nature of the zirconium–phosphorus bonding. Careful examination of the structural parameters of **1** establishes that the Dmp(H)P group of **1** is essentially intermediate to the two limiting types of Dmp(H)P groups in **2**. Firstly, the Zr–P bond length of $2.638(1)$ Å of **1** is close to the average Zr–P distances in **2** (2.622 Å). Secondly, a flattened pyramidal geometry for the phosphanido ligand in **1** is indicated by the sum of the bond angles at the phosphorus atom ($\Sigma_{\text{BA}}(\text{P}) = 331(3)^\circ$), which is also close to the average of the two corresponding values in **2** (average $\Sigma_{\text{BA}}(\text{P}) = 335^\circ$). Lastly, the Zr–P–C bond angle of $125.7(1)^\circ$ in **1** is between the two corresponding values for **2**. As such,

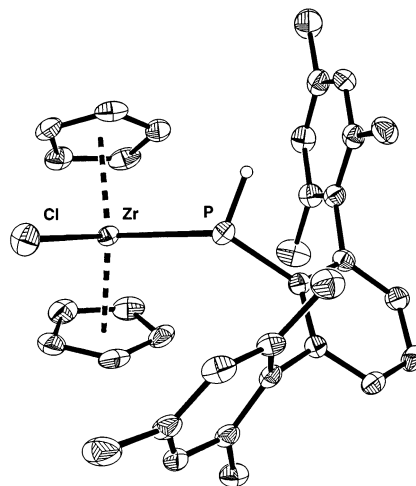


Fig. 2. Thermal ellipsoid plot for $[\text{Cp}_2\text{Zr}(\text{Cl})(\text{P}(\text{H})\text{Dmp})]$ (**1**). Selected bond distances (Å) and angles ($^\circ$): Zr–P: $2.638(1)$, Zr–Cl: $2.449(1)$, P–Cl: $1.841(4)$, P–H: $1.29(5)$, P–Zr–Cl: $97.05(4)$, H–P–Zr: $104(2)$, Cl–P–Zr: $125.7(1)$, H–P–Cl: $101(2)$.

the Dmp(H)P group of compound **1** models, at least in the solid state, the transition state for interconversion of the two types of phosphanido groups of **2**.

Table 2 lists the key structural features of some related structurally characterized Zr(IV) metallocene complexes having a single terminal phosphanido ligand. Analysis of these data reveals some interesting facts. First, a range of geometries is observed for the phosphorus centers, ranging from essentially planar to pyramidal geometries. A rough correlation appears to exist between the steric congestion about each phosphorus center and the metal–phosphorus bond lengths. For example, the complex having the most congested phosphorus center, $[\text{Cp}_2\text{Zr}(\text{Cl})\{\text{P}(\text{SiMe}_3)\text{Mes}^*\}]$, contains the shortest Zr–P bond length. The shorter M–P distances also scale with the planarity of the phosphanido ligand. Increasing rehybridization to a planar geometry would allow the phosphorus centers to engage in increased π -bonding to the metal center. It is well known, however, that phosphorus(III) resists structural rearrangements from pyramidal to planar [31]. The data from Table 2 suggest that such a rehybridization at phosphorus may be facilitated by steric congestion. No correlation between Zr–P and Zr–Cl bond distances is readily discerned that would allow a dissection of po-

Table 2
Selected structurally characterized zirconocene(IV) and hafnocene(IV) terminal mono-phosphanido complexes

Phosphanido complexes	d_{MP} (Å)	d_{MX} (Å)	$^{31}\text{P}\{^1\text{H}\}$ NMR	$\Sigma_{\text{BA}}(\text{P})$ (°)	P–Zr–X angle (°)	Ref.
$[\text{Cp}_2\text{Zr}(\text{Cl})\{\text{P}(\text{SiMe}_3)\text{Mes}^*\}]$	2.541(4)	2.485	156	359.5 (0.7)	100.39	[55]
$[\text{Cp}_2\text{Zr}(\text{Cl})\{\text{P}(\text{H})\text{Mes}^*\}]$	2.543(3)	2.494(3)	83.2	350.5	98.61(9)	[35]
$[\text{Cp}_2\text{Zr}(\text{Cl})\{\text{P}(\text{SiMe}_3)_2\}]$	2.547(6)	2.432(5)	–108.9	344.4 (0.8)	100.6(4)	[56]
$[\text{Cp}^*_2\text{Hf}(\text{H})\{\text{P}(\text{H})\text{Ph}\}]^a$	2.549(8)	^b	30.5	^b	^b	[57]
$[\text{Cp}_2\text{Zr}(\text{CH}_3)\{\text{P}(\text{SiMe}_3)_2\}]$	2.629(3)	2.35(6)	–121.7	349.2 (0.3)	98(1)	[56,61]
$[\text{Cp}_2\text{Zr}(\text{Cl})\{\text{P}(\text{H})\text{Dmp}\}]$ (1)	2.638(1)	2.449(1)	25.0	330.7 (2.8)	97.05(4)	this work
$[\text{Cp}'_2\text{Zr}(\text{Cl})\{\text{P}(\text{H})\text{Trip}\}]^c$	2.6381(8)	2.4547(6)	–4.6	328.6 (2.0)	93.55(2)	[58]
$[\text{Cp}_2^0\text{Zr}(\text{Cl})\{\text{P}(\text{H})\text{Cy}\}]^d$	2.6539(9)	2.4442(9)	71.7	308 (2)	99.79(4)	[59]

^a Cp* = C₅Me₅.

^b Data unavailable owing to structural disorder.

^c Cp' = C₅H₄Me, Trip = 2,4,6-ⁱPr₃C₆H₂.

^d Cp⁰ = C₅EtMe₄.

tential competing π -bonding between zirconium from chloride or phosphorus. Oddly, exchange of chloride for methyl in $[\text{Cp}_2\text{Zr}(\text{Cl})\{\text{P}(\text{SiMe}_3)_2\}]$ lengthens the Zr–P bond length (0.082 Å), while effecting little change in the geometry of the phosphorus atom. Interestingly, exchange of phosphorus for arsenic in $[\text{Cp}_2\text{Zr}(\text{Cl})\{\text{E}(\text{SiMe}_3)_2\}]$ (E = P, As) results in a significant change in ligand geometry from $\Sigma_{\text{BA}}(\text{P}) = 344.4^\circ$ to $\Sigma_{\text{BA}}(\text{As}) = 328.8^\circ$ ($d_{\text{ZrCl}} = 2.445(1)$ Å, $d_{\text{ZrAs}} = 2.7469(7)$ Å) [32]. Such an effect may be the result of the larger covalent radius of arsenic, and hence, a more relaxed steric environment at the arsenic center as compared to the phosphorus center.

The above analysis would also imply that the electronically favored geometry for zirconocene phosphanido groups is pyramidal and that zirconium–phosphorus π -bonding alone is not a sufficient driving force for planarization of phosphanido ligands. Barrier heights for pyramidal inversion at phosphorus in the hypothetical species $[\text{Cp}_2\text{Ti}(\text{Cl})\text{PR}_2]$ [33]³ have been calculated using the approximate molecular orbital method partial retention of diatomic differential overlap (PRDDO) [34]. Stabilization of a planar phosphorus geometry by ligand-to-metal π -bonding was suggested to facilitate the inversion process. A barrier height of 6.7 kcal mol^{–1} was found for $[\text{Cp}_2\text{Ti}(\text{Cl})\text{PH}_2]$ ($\Sigma_{\text{BA}}(\text{P}) = 305.6^\circ$ for pyramidal geometry), while for $[\text{Cp}_2\text{Ti}(\text{Cl})\{\text{P}(\text{H})\text{Ph}\}]$ and $[\text{Cp}_2\text{Ti}(\text{Cl})\text{PPH}_2]$ a planar phosphanido ligand was predicted to be favored over a pyramidal phosphanido group. The latter results were ascribed to the phenyl groups being bulkier than hydrogens and the ability of the phenyl groups to find resonance stabilization with the P-atom lone pair. Our preliminary calculations using density functional theory [18,21] on $[\text{Cp}_2\text{Zr}(\text{X})\text{PH}_2]$ also show a preference for pyramidal phosphanido groups. Energy minimization of a model

complex $[\text{Cp}_2\text{Zr}(\text{Cl})\text{PH}_2]$ produced a geometry for $[\text{Cp}_2\text{Zr}(\text{Cl})\text{PH}_2]$ having a pyramidal PH₂ group ($\Sigma_{\text{BA}}(\text{P}) = 286.3^\circ$) and Zr–P and Zr–Cl bond distances of 2.669 and 2.450 Å, respectively. Minimization of $[\text{Cp}_2\text{Zr}(\text{H})\text{PH}_2]$ also favored a complex having a pyramidal PH₂ unit ($\Sigma_{\text{BA}}(\text{P}) = 293.9^\circ$) with Zr–P and Zr–H bond distances of 2.656 and 1.856 Å, respectively. Minimization of $[\text{Cp}_2\text{Zr}(\text{Cl})\text{PH}_2]$ while constraining the PH₂ unit to a planar geometry led to a structure 6.8 kcal mol^{–1} higher in energy than the structure having a pyramidal PH₂ group and led to $d_{\text{ZrP}} = 2.520$ Å and $d_{\text{ZrCl}} = 2.498$ Å.

The crystal structure of $[\text{Cp}_2\text{Zr}(\text{Cl})\{\text{P}(\text{H})\text{Mes}^*\}]$ [35] (**4**, Mes* = 2,4,6-ⁱBu₃C₆H₂) allows a direct comparison of the influence of the aryl groups on the geometry of the phosphanido groups for two $[\text{Cp}_2\text{Zr}(\text{Cl})\{\text{P}(\text{H})\text{Ar}\}]$ complexes. The Zr–P bond length of 2.543(3) Å in **4** is shorter than the same bond length in **1**. The Zr–P–C angle of 128.4(2)° in **4** is slightly smaller than the analogous angle in **1**. A somewhat planar geometry for the Mes*(H)P group in **4** is suggested by the sum of the bond angles at phosphorus ($\Sigma_{\text{BA}}(\text{P}) = 350^\circ$) and corroborated by a shorter Zr–P bond distance. A greater degree of planarity for **4** compared to **1** is consistent with previous arguments that a single Mes* group imposes greater steric distortions than a single Dmp group [36].

The phosphanido group of **1** is approximately an average of the two types of phosphanido groups of **2**. No such relationship connects the structures of **4** and $[\text{Cp}_2\text{Zr}\{\text{P}(\text{H})\text{Mes}^*\}_2]$ (**5**) [23]. For example, compound **5** contains two longer and nearly identical Zr–P bond lengths of 2.681(5) and 2.682(5) Å. The two Zr–P–C bond angles in **5** of 119.0(3) and 119.3(3)° are smaller than the value for **4**. Based on this information, the geometry at each phosphanido group of **5** would thus be expected to be identical, but differences in the sum of the bond angles at each phosphorus center in **5** ($\Sigma_{\text{BA}}(\text{P}) = 321(2)$ and $356(2)^\circ$) would suggest the presence of two types of phosphanido groups. Owing to the

³ The first example of a structurally characterized simple Ti(IV) phosphanido complex has recently been reported (see Ref. [33]).

Table 3
Selected structurally characterized zirconocene(IV) and hafnocene(IV) terminal bis-phosphanido complexes

Phosphanido complexes	d_{MP} (Å)	$^{31}\text{P}\{^1\text{H}\}$ NMR	$\Sigma_{\text{BA}}(\text{P})$ (°)	P–Zr–P angle (°)	Ref.
$[\text{Cp}_2\text{Hf}\{\text{PEt}_2\}_2]$	2.488(1), 2.682(1)	–	358.8 (0.3), 311.9 (0.3)	98.64(3)	[29]
$[\text{Cp}_2\text{Zr}\{\text{P}(\text{H})\text{Dmp}\}_2]$ (2)	2.519(2), 2.726(2)	17.4	357.8 (5.7), 301.4 (4.2)	91.30(7)	this work
$[(\text{C}_5\text{H}_4\text{SiMe}_3)_2\text{Zr}\{\text{PPh}_2\}_2]$	2.536(3), 2.694(3)	144.1	359.9 (0.6), 326.5 (0.6)	103.75(9)	[60]
$[\text{Cp}_2\text{Hf}\{\text{P}(\text{SiMe}_3)_2\}]$	2.553(1), 2.654(1)	–98.8	360.0 (0.2), 336.0 (0.2)	99.4(1)	[61]
$[\text{Cp}'_2\text{Zr}\{\text{P}(\text{SiMe}_3)_2\}]^a$	2.600(2), 2.634(2)	–71.2	358.3 (0.1), 351.2 (0.1)	96.95(7)	[62]
$[\text{Cp}^*_2\text{Zr}\{\text{P}(\text{H})\text{Mes}\}_2]^b$	2.63(2)	39.0	^c	96.1(7)	[27]
$[\text{Cp}_2\text{Zr}\{\text{P}(\text{H})\text{Mes}^*\}_2]$	2.681(5), 2.682(5)	51.6	356.0 (2.8), 321.3 (2.8)	97.86(9)	[23]

^a Cp' = C₅H₄Me.

^b Cp* = C₅Me₅, Mes = 2,4,6-Me₃C₆H₂.

^c Hydrogen atoms not located.

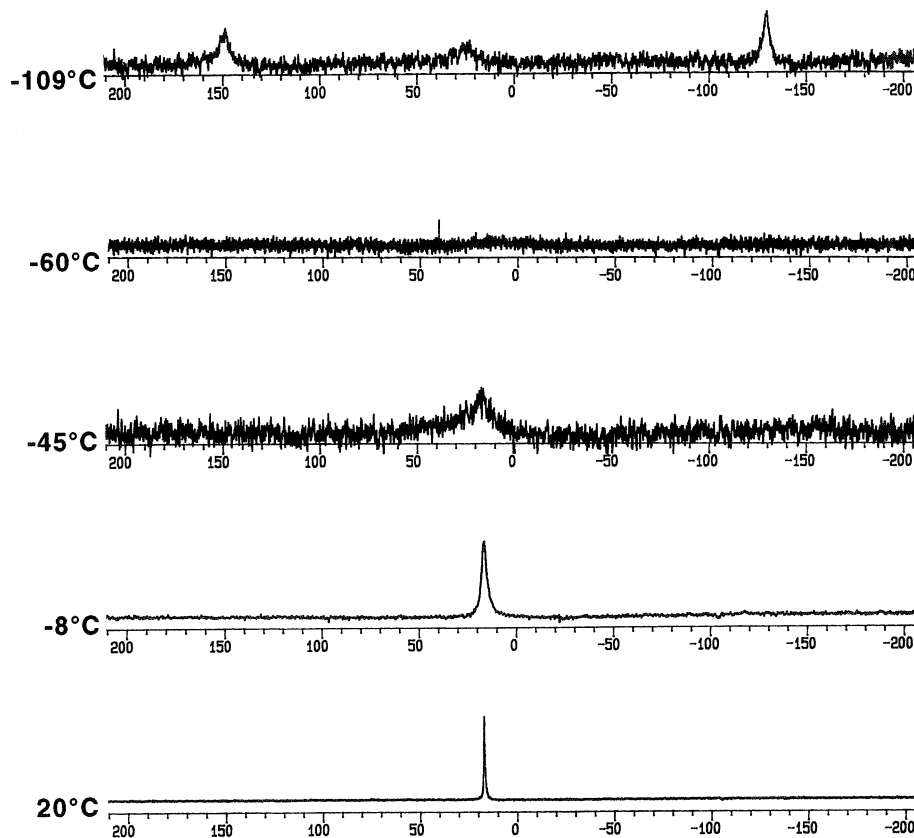


Fig. 3. Variable temperature $^{31}\text{P}\{^1\text{H}\}$ NMR (toluene) of $[\text{Cp}_2\text{Zr}\{\text{P}(\text{H})\text{Dmp}\}_2]$ (**2**).

lower quality of the structure of **5** ($R = 0.098\%$) the hydrogen atom positions may not be well defined.

Regardless, the relationship between **4** and **5** is very different than that between **1** and **2**. As pointed out previously, π -bonding between a phosphanido group and zirconium will require the group to reorient itself so that the phosphorus p orbital can donate to the a_1 π -accepting molecular orbital of the metallocene fragment. Steric interactions in **5** between the two bulky Mes*(H)P groups may be responsible for preventing the alignment of one of the two groups for π -bonding.

Although the steric shielding provided by Dmp and Mes* groups are close to one another, they differ somewhat in the three-dimensional form of their screening. Both types of systems have been successfully employed to stabilize unusual environments involving main group elements [37–41]. The particular steric demands of the Dmp and Mes* ligands at metal centers have been contrasted, and it has been suggested that introduction of two bulky aryls (MAR_2) produces greater steric congestion and geometrical distortions for compounds containing two Dmp ligands as compared

to complexes containing two Mes* groups [36,42,43]. The aryl groups of **2** and **5** are more insulated from one another and connected by three atoms as opposed to a single atom, however. A potentially better comparison to a pair of iron(II) bis-thiolate complexes bearing both kinds of hindered aryls is clouded by the fact that the Mes* containing species is dimeric ($\{Mes^*S\}_2Fe\}_2$) and the Dmp containing species is monomeric $\{DmpS\}_2Fe$ [44,45]. Comparisons can also be drawn to phosphorus atoms double bonded directly to one another in the diphosphenes $DmpP=PDmp$ and $Mes^*P=PMes^*$. The P=P bond length in the former material is slightly shorter than in the latter (1.985(2) vs. 2.034(2) Å) suggesting that a closer approach of two DmpP units is easier than for two Mes*P units [17,46]. A full analysis will require additional structural determinations.

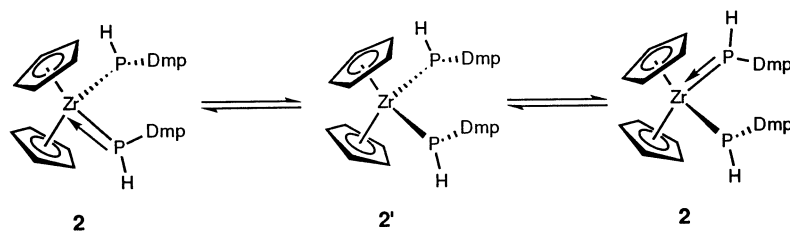
Further data for some Zr(IV) and Hf(IV) metallocenes bearing two terminal phosphanido ligands are presented in Table 3. A greater range of M–P bond lengths and ligand geometries is observed for these complexes than in analogous mono-phosphanido species. Again, the phosphanido groups displaying shorter M–P bonds are more planar. As observed for the mono-phosphanido complexes, as the phosphorus centers become increasingly planar, the metal–phosphorus bond lengths decrease. Notably, the range of metal–phosphorus bond lengths spans a greater range of values for the bis-phosphanido complexes than for the mono-phosphanido complexes. The less direct correlation of sterics to the type of bonding mode for bis-phosphanido metallocenes may reflect the difficulty for a planar phosphanido group to orient itself so that the phosphorus p-orbital may be in alignment to the a_1 π -accepting molecular orbital of the metallocene fragment, as proposed for $[Cp^*Zr\{P(H)Mes^*\}_2]$ [8,24–27]. Further computational studies will be needed to examine these issues.

The fascinating display of two types of phosphanido groups in **2** in the solid state is shared by several of the other complexes in Table 3. Detecting this phenomenon in solution however is not always possible. Low-temperature ^{31}P NMR studies of $[Cp_2Hf(PEt_2)_2]$, for example, revealed a single time-averaged signal even upon cooling. Replacing the diethylphosphanido groups by more bulky dicyclohexylphosphanido groups allowed

the process which interconverts the two type of phosphanido groups to be observed on the NMR time-scale at $-126^\circ C$ (δ 270.2 and -15.3 ppm) (Scheme 3) [29].

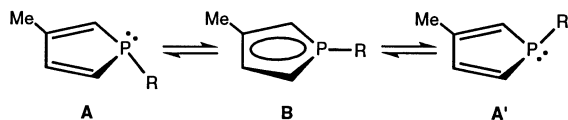
The asymmetry of the phosphanido groups of **2** in solution is also not evinced by room temperature $^{31}P\{^1H\}$ NMR spectroscopy. Upon cooling the resonance broadens and at about $-60^\circ C$ disappears into the baseline (Fig. 3). At about $-109^\circ C$ very broad signals centered at δ 149, 25 and -130 ppm appear in an approximate 0.36:0.30:0.34 ratio. Calculation of the weighted chemical shift for this distribution of species gives δ 17, in exact agreement with the room temperature shift for **2**. Solubility problems prevented further measurements at reduced temperatures. The signals of equal magnitude at δ 149 and -130 are assigned to the planar and pyramidal phosphorus atoms of **2**, respectively [1]. The signal at δ 25 is tentatively assigned as a second isomer of **2** (**2'**, Scheme 4) having two equivalent Dmp(H)P groups with geometries comparable to those found in **1** ($^{31}P\{^1H\}$ NMR: δ 25). Thus, compound **2**, unlike other structurally characterized metallocene(IV) bis-phosphanido complexes, appears to have a delicate balance of steric and electronic forces to afford significant concentrations of the two forms of **2**. Both isomers **2** and **2'** could have stereoisomers, owing to the presence of chiral pyramidal phosphanido groups [8,24–27], but the range of chemical shifts is probably too large to be explained by such stereoisomers. Low-temperature ^{31}P NMR spectroscopy of $[Cp_2Zr\{P(H)Mes^*\}_2]$ showed only a single resonance down to $-80^\circ C$ [23]. Variable-temperature 1H NMR, however, did show evidence for hindered P–C bond rotation and inversion at phosphorus.

The importance of steric congestion for inducing planar geometries and π -bonding for P(III) has been previously noted in the chemistry of phospholes. These five-membered heterocycles (below) might be expected to be aromatic if a planar geometry is adopted by the phosphorus center. The phospholes that exhibit the greatest degree of aromaticity and the lowest barriers to pyramidal inversion (interconversion of **A** and **A'**), however, are the ones containing the most sterically demanding groups (such as $R = Mes^*$) [47,48]. The role of extreme sterics has been further noted in select phosphametallacycles where delocalization of the phosphorus lone pair is unlikely [25,49,50]. On the other



Scheme 4.

hand, pyramidal inversion of phosphines can be promoted by main group Lewis acids by a mechanism involving backside attack of empty p-orbital of the main group species on the smaller lobe of the phosphorus lone pair. However, this inversion leads to coordination of the phosphorus center (see Ref. [50]).



The conclusion suggested by the above analyses is that zirconium(IV) or hafnium(IV) metallocenes containing planar phosphanido groups may require the assistance of sterically encumbering group(s) to persuade the phosphorus center to adopt an undesired planar geometry. The zirconium or hafnium center may take advantage of this situation and engage in π -bonding to the now planarized phosphanido group. This effect may be tempered in complexes of the form $[\text{Cp}_2\text{Zr}\{\text{PRR}'\}_2]$ if the presence of the second phosphanido group sterically hinders adoption of the proper orientation for Zr–P π -bonding to occur. Previous descriptions of the bonding of phosphanido ligands to metal centers have emphasized only the importance of the metal center to achieve an 18-electron valence configuration. It must also be remembered that while phosphorus(III) resists structural rearrangements from pyramidal to planar, planar geometries for amido ligands are the norm [51–54]. Planar metal amides, however, do not necessarily mandate N–M p-d π -bonding [54].

4. Supplementary material

Full experimental details for the X-ray crystallographic analysis of **1** and **2**. Crystallographic data for the structural analysis has been deposited with the Cambridge Crystallographic Data Centre. Copies of this information may be obtained free of charge from: The Director, CCDC, 12 Union Road, Cambridge, CB2 1EZ, UK (fax: +44-1223-336-033; email: deposit@ccdc.cam.ac.uk or www: <http://www.ccdc.cam.ac.uk>).

Acknowledgements

We thank the National Science Foundation (CHE-9733412) and the Department of Chemistry at CWRU for support of this work. J.D.P. also wishes to acknowledge Professor Stephen J. Lippard for his invaluable crystallographic lessons and for sharing his passion for relating chemical structure to chemical function and reactivity.

References

- [1] E. Hey-Hawkins, *Chem. Rev.* 94 (1994) 1661–1717.
- [2] D.W. Stephan, *Coord. Chem. Rev.* 95 (1989) 41–107.
- [3] N. Etkin, M.C. Fermin, D.W. Stephan, *J. Am. Chem. Soc.* 119 (1997) 2954–2955.
- [4] M.C. Fermin, D.W. Stephan, *J. Am. Chem. Soc.* 117 (1995) 12645–12646.
- [5] D.W. Stephan, *Angew. Chem.*, in press.
- [6] A.H. Cowley, *Acc. Chem. Res.* 30 (1997) 445–451.
- [7] T.L. Breen, D.W. Stephan, *Organometallics* 16 (1997) 365–369.
- [8] T.L. Breen, D.W. Stephan, *J. Am. Chem. Soc.* 117 (1995) 11914–11921.
- [9] J.B. Bonanno, P.T. Wolczanski, E.B. Lobkovsky, *J. Am. Chem. Soc.* 116 (1994) 11159–11160.
- [10] C.C. Cummins, R.R. Schrock, W.M. Davis, *Angew. Chem., Int. Ed. Eng.* 32 (1993) 756–759.
- [11] A.H. Cowley, A.R. Barron, *Acc. Chem. Res.* 21 (1988) 81–87.
- [12] F. Mathey, *Angew. Chem., Int. Ed. Eng.* 26 (1987) 275–286.
- [13] G. Huttner, K. Evertz, *Acc. Chem. Res.* 19 (1986) 406–413.
- [14] E. Urnėžius, J.D. Protasiewicz, manuscript in preparation.
- [15] G.W. Rabe, S. Kheradmandan, L.M. Liable-Sands, I.A. Guzei, A.L. Rheingold, *Angew. Chem., Int. Ed. Eng.* 37 (1998) 1404–1407.
- [16] G.W. Rabe, S. Kheradmandan, G.P.A. Yap, *Inorg. Chem.* 37 (1998) 6541–6543.
- [17] E. Urnėžius, J.D. Protasiewicz, *Main Group Chem.* 1 (1996) 369–372.
- [18] A.D. Becke, *J. Chem. Phys.* 98 (1993) 5648–5652.
- [19] W.J. Hehre, L. Radom, P.P. Schleyer, J.A. Pople, *Ab Initio Molecular Orbital Theory*, Wiley, New York, 1986.
- [20] P.J. Hay, W.R. Wadt, *J. Chem. Phys.* 82 (1985) 299–310.
- [21] M.J. Frisch, H.B. Schlegel, P.M.W. Gill, B.G. Johnson, M.A. Robb, J.R. Cheeseman, T. Keith, G.A. Petersson, J.A. Montgomery, K. Raghavachari, M.A. Al-Laham, V.G. Zakrzewski, J.V. Ortiz, J.B. Foresman, J. Cioslowski, B.B. Stefanov, A. Nanayakkara, M. Challacombe, C.Y. Peng, P.Y. Ayala, W. Chen, M.W. Wong, J.L. Andres, E.S. Replogle, R. Gomperts, R.L. Martin, D.J. Fox, J.S. Binkley, D.J. Defrees, J. Baker, J.J.P. Stewart, M. Head-Gordon, C. Gonzalez, J.A. Pople, *GAUSSIAN 94*, Revision C.3, Gaussian, Pittsburgh, PA, 1995.
- [22] S.R. Wade, M.G.H. Wallbridge, G.R. Willey, *J. Chem. Soc., Dalton Trans.* (1983) 2555–2559.
- [23] E. Hey-Hawkins, S. Kurz, *J. Organomet. Chem.* 479 (1994) 125–133.
- [24] T.L. Breen, D.W. Stephan, *Organometallics* 15 (1996) 4223–4227.
- [25] T.L. Breen, D.W. Stephan, *J. Am. Chem. Soc.* 118 (1996) 4204–4205.
- [26] T.L. Breen, D.W. Stephan, *Organometallics* 15 (1996) 4509–4514.
- [27] Z. Hou, T.L. Breen, D.W. Stephan, *Organometallics* 12 (1993) 3158–3167.
- [28] E. Urnėžius, J.D. Protasiewicz, unpublished results.
- [29] R.T. Baker, J.F. Whitney, S.S. Wreford, *Organometallics* 2 (1983) 1049–1051.
- [30] (a) M.C. Kuchta, G. Parkin, *Coord. Chem. Rev.* 176 (1998) 323–372. (b) K.G. Caulton, *New J. Chem.* 18 (1994) 25–41.
- [31] W. Kutzelnigg, *Angew. Chem., Int. Ed. Eng.* 23 (1984) 272–295.
- [32] E. Hey-Hawkins, F. Lindenberg, *Organometallics* 13 (1994) 4643–4644.
- [33] A.V. Firth, D.W. Stephan, *Inorg. Chem.* 37 (1998) 4732–4734.
- [34] J.R. Rogers, T.P.S. Wagner, D.S. Marynick, *Inorg. Chem.* 22 (1994) 3104–3110.
- [35] J. Ho, R. Rousseau, D.W. Stephan, *Organometallics* 13 (1994) 1918–1926.

- [36] R.S. Simons, L. Pu, M.M. Olmstead, P.P. Power, *Organometallics* 16 (1997) 1920–1925.
- [37] A.H. Cowley, N.C. Norman, *Prog. Inorg. Chem.* 34 (1986) 1–63.
- [38] P.J. Brothers, P.P. Power, in: R. West, F.G.A. Stone (Eds.), *Multiply Bonded Main Group Metals and Metalloids*, Academic Press, San Diego, CA, 1996, pp. 1–63.
- [39] A.H. Cowley, *J. Organomet. Chem.* 400 (1990) 71–80.
- [40] N.C. Norman, *Polyhedron* 12 (1993) 2431–2446.
- [41] P.P. Power, *J. Chem. Soc., Dalton. Trans.* (1998) 2939–2951.
- [42] X.-W. Li, W.T. Pennington, G.H. Robinson, *Organometallics* 14 (1995) 2109–2111.
- [43] R.J. Wehmschulte, W.J. Grigsby, B. Schiemenz, R.A. Bartlett, P.P. Power, *Inorg. Chem.* 35 (1996) 6694–6702.
- [44] P.P. Power, S.C. Shoner, *Angew. Chem., Int. Ed. Eng.* 30 (1991) 330–332.
- [45] J.J. Ellison, K. Ruhlandt-Senge, P.P. Power, *Angew. Chem., Int. Ed. Eng.* 33 (1994) 1178–1180.
- [46] M. Yoshifuji, I. Shima, N. Inamoto, K. Hirotsu, T. Higuchi, *J. Am. Chem. Soc.* 103 (1981) 4587–4589.
- [47] G. Keglevich, Z. Böcskei, G.M. Keserü, K. Ujszászy, L.D. Quin, *J. Am. Chem. Soc.* 119 (1997) 5095–5099.
- [48] L. Nyulászi, L. Soós, G. Keglevich, *J. Organomet. Chem.* 566 (1998) 29–35.
- [49] T.L. Breen, D.W. Stephan, *Organometallics* 15 (1996) 5729–5737.
- [50] M.D. Fryzuk, G.R. Giesbrecht, S.J. Rettig, *Inorg. Chem.* 37 (1998) 6928–6934.
- [51] M.A. Dewey, D.A. Knight, A. Arif, J.A. Gladysz, *Chem. Ber.* 125 (1992) 815–824.
- [52] S.C. Goel, M.Y. Chiang, D.J. Rauscher, W.E. Buhro, *J. Am. Chem. Soc.* 115 (1993) 160–169.
- [53] M.A. Matchett, M.Y. Chiang, W.E. Buhro, *Inorg. Chem.* 33 (1994) 1109–1114.
- [54] M.F. Lappert, P.P. Power, A.R. Sanger, R.C. Srivastava, *Metal and Metalloid Amides*, Wiley, New York, 1980.
- [55] A.M. Arif, A.H. Cowley, C.M. Nunn, M. Pakulski, *J. Chem. Soc., Chem. Commun.* (1987) 994–995.
- [56] E. Hey, M.F. Lappert, J.L. Atwood, S.G. Bott, *Polyhedron* 7 (1988) 2083–2086.
- [57] G.A. Vaughan, G.L. Hillhouse, A.L. Rheingold, *Organometallics* 8 (1989) 1760–1765.
- [58] E. Hey-Hawkins, S. Kurz, G. Baum, *Z. Naturforsch., Teil B* 50 (1995) 239–242.
- [59] U. Seeger, E. Hey-Hawkins, *Polyhedron* 16 (1997) 2537–2545.
- [60] A.-M. Larsonneur, R. Choukroun, J.-C. Daran, T. Cuenca, J.C. Flores, P. Royo, *J. Organomet. Chem.* 444 (1993) 83–89.
- [61] L. Weber, G. Meine, R. Boese, N. Augart, *Organometallics* 6 (1987) 2484–2488.
- [62] F. Lindenberg, E. Hey-Hawkins, *J. Organomet. Chem.* 435 (1992) 291–297.